Locally and Temporally Adaptive Clutter Removal in Weather Radar Measurements

Jörn Sierwald[1] and Jukka Huhtamäki[1]

[1]*Eigenor Corporation, Lompolontie 1, 99600 Sodankylä, Finland*

(Dated: 27 June 2014)

1. Introduction

We present a method of mitigating ground clutter selectively from a weather radar measurement. The clutter removal varies both from bin to bin and from scan to scan, and is therefore a locally and temporally adaptive algorithm. In the following, we will first briefly describe the underlying idea behind the method and how to remove a ground clutter component from a weather radar signal. After the technical discussion, a few illustrative results are shown how the algorithm performs in a real weather event.

The main motivation of adaptive ground clutter mitigation is to avoid unnecessary artifacts in meteorological products due to clutter filtering. The strength of the clutter signal often varies significantly from one bin to the other, especially within urban regions. For a chosen bin, it also differs from scan to scan, for example, due to changing weather conditions. A rudimentary algorithm which blindly applies a single clutter filter across the entire measurement volume often acts too aggressively on regions which contain weak or no ground clutter component and too weakly on severely contaminated bins. These effects result in suppressed meteorological reflectivity and residual clutter signals, respectively. With the current algorithm even small traces of ground clutter, which may deteriorate polarimetric products (Friedrich et al., 2009), can be removed.

For adaptive clutter removal, an automatic mechanism is needed which decides what kind of clutter filter is needed for a given bin. In our algorithm, this decision is based on dual-polarization analysis of the signal: First, a given raw data signal is filtered using several chosen filters which can be, for example, of varying strength. Dual-polarization products are calculated for each processed signal. Based on several factors including the polarimetric data, and in particular how they change from one filter to the next, one can decide the weakest filter which is capable of mitigating a possible clutter component.

Our algorithm can be compared to a previously studied adaptive ground clutter mitigation technique. GMAP (Gaussian model adaptive processing) (Siggia and Passarelli, 2004) is a well-known clutter removal algorithm often used in uniformly pulsed Doppler measurements. This system is adaptive in the sense that it automatically removes more for strong clutter components based on a Gaussian clutter model. Moreover, this system can be combined with a decision-making method, for example CMD (clutter mitigation decision) (Hubbert et al., 2009). Based on the dual-polarization characteristics of the input signal, CMD attempts to directly decide whether it is contaminated with ground clutter or not. The major differences compared to our approach are: (1) our filtering is carried out in the time domain and is specifically constructed to cope with arbitrary pulsing schemes (such as uniform pulsing, staggered PRT and triple-PRT (Tabary et al., 2006)) and (2) the decision-making part is based principally on how the filtering affects the signal instead of a direct observation based on estimated products.

The algorithm is tested with measurements made by the Kumpula Radar at University of Helsinki. We have chosen to use a triple-PRT pulsing scheme where pulses are sent in patterns consisting of three different intervals: 1750, 2000, and 2500 milliseconds. Non-uniform pulsing is used in order to surpass the range–Doppler dilemma: with the C-band radar we are capable of measuring velocities up to 53.5 m/s with an operating range of 262.5 km.

2. Method

A more detailed description of the ground clutter removal technique can be found from (Sierwald and Huhtamäki, 2014). A partial recap of the method can also be found from (Sierwald and Huhtamäki, 2013).

2.1. Ground Clutter Filter

Ground clutter is filtered directly from the input I/Q signal through a matrix multiplication. For now, we approximate that the ground clutter auto-correlation function has a Gaussian functional form [1]. Assuming that the signal is a sum of ground clutter and white noise with power P_n, based on statistical inversion theory, it can be shown that the optimal matrix filter is given by

$$G = \left(I + \frac{R_{gc}}{P_n}\right)^{-1},$$

(2.1)

---

[1]This is not the optimal model in some cases. For example with moving vegetation, an exponential form is more accurate.

where R_{gc} is the covariance matrix of the ground clutter. G is the most optimal clutter filter matrix in the sense that multiplication with it subtracts the most likely clutter component, or the so-called posteriori expectation value of the clutter signal, from the original signal. A benefit of this approach is that it works for an arbitrary pulsing scheme. Information on the pulse timings enters the algorithm through the covariance matrix R_{gc}. Strength of the clutter filter is controlled through a single parameter: the ratio of clutter power to noise power. The filter matrix is similar to the one used in the GMAT algorithm (Nguyen et al., 2008) with the relation $G = G_{\text{GMAT}}^2$.

2.2. Adaptive Filtering

Figure 1 summarizes the process of adaptive filtering. Multiplication of the input signal with a matrix is computationally a relatively cheap operation. The input signal can be processed with several filters within restrictions of real-time operation. The decision-making system attempts to choose the weakest filter capable of mitigating the ground clutter component based on the following checks

- Value of $\text{ACF}(T_{\text{pattern}})$, where T_{pattern} is the total time interval of a complete pulsing cycle.
- Variability of the copolar differential phase Ψ_{dp} over range.
- Power variability over range and azimuth.
- Power loss due to filtering.
- Linear regression analysis of Ψ_{dp} using filtered data.
- Receiver saturation check.
- Value of the copolar correlation coefficient ρ_{co} and its change in filtering.
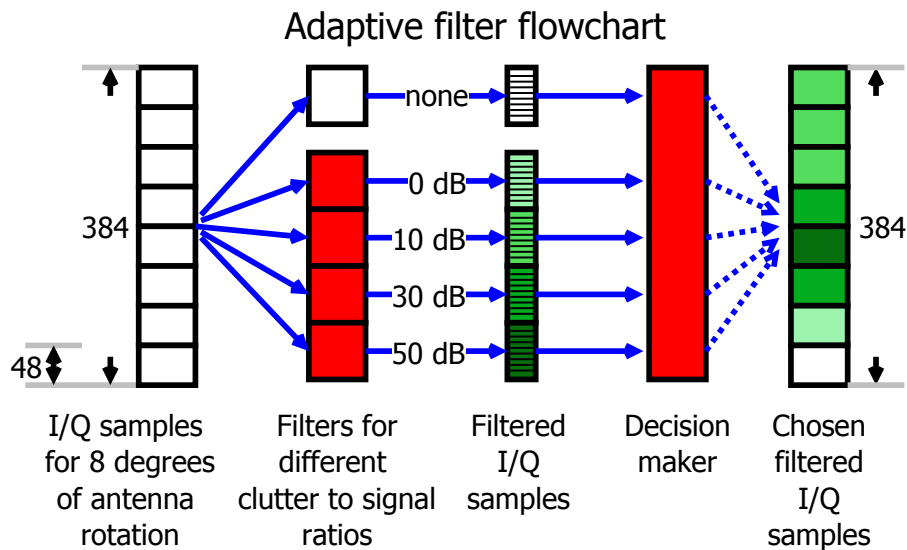- Result of the decision algorithm for neighboring gates.

Figure 1: The ground clutter removal algorithm processes a chunk of 8 azimuthal degrees of data. In this example, this translates to 384 time series samples for each range gate. Several ground clutter filters, for example of different strength, are applied to the input signal. The decision-making step chooses filtered signals which correspond the best to the nature of precipitation signals for further analysis.

3. Results

The measurements were made using the Kumpula Radar located at University of Helsinki. It is a C-band ($\lambda = 5.35$ cm) Vaisala weather radar equipped with a klystron transmitter and an RVP900 signal processor. The measurements were made using the receiver's wide dynamic range setup. As shown in Figure 2, the radar is located in the metropolitan region of Finland. Low-elevation scans typically contain clutter from various sources, including traffic, constructions and terrain. Some regions close to the radar contain ground clutter strong enough to saturate the receiver and several areas reach levels above the phase-noise figure of the system (roughly 50–55 dB) which places a hard limit for clutter removal.
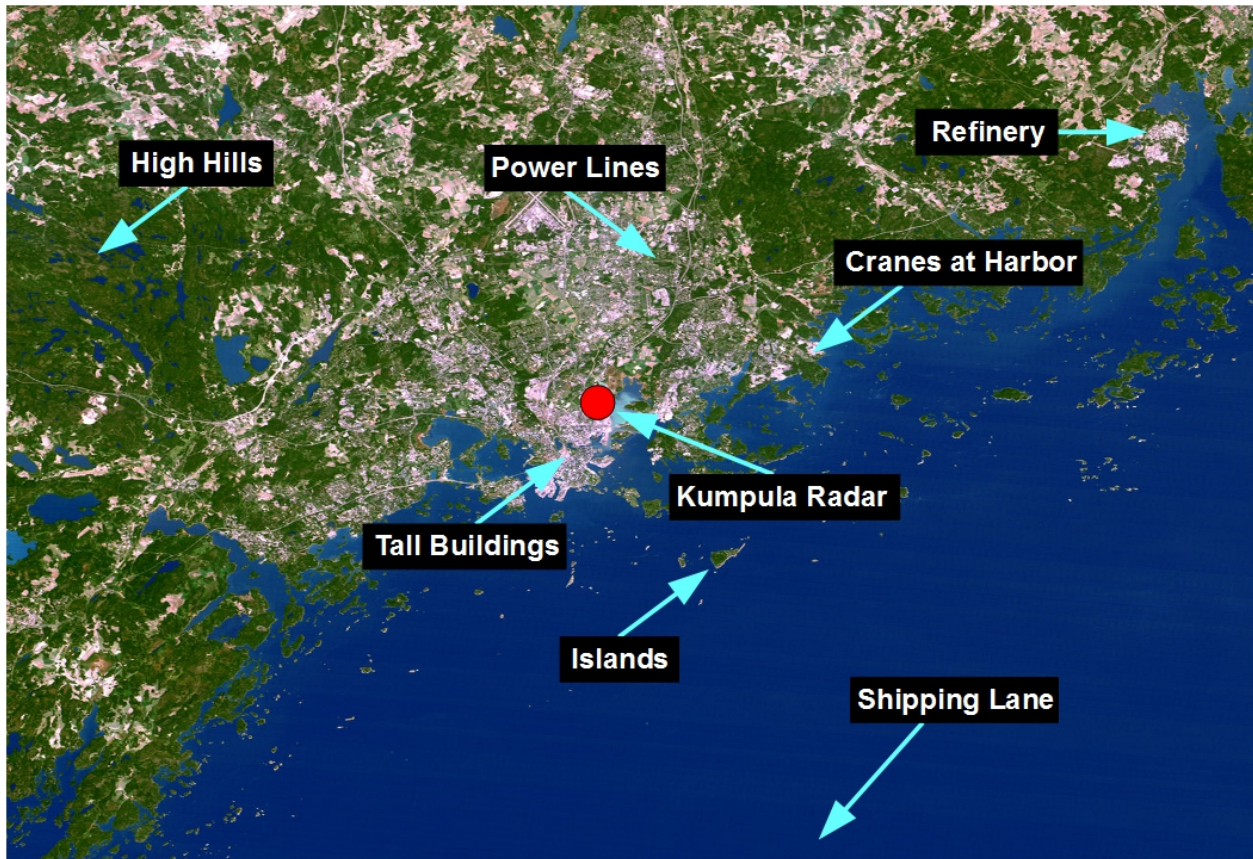
Figure 2: Most prominent clutter targets visible with the Kumpula Radar.

Figure 3 illustrates adaptive filtering with a clear-sky measurement at sunrise in September 2013. The received power in Figure 3 (a) clearly shows all the stationary ground clutter targets pointed out in Figure 2. The rays to the south are sea clutter from a stationary sea surface. Reflectivity (power after clutter filtering) is shown in Figure 3 (b). The remaining reflectivity within the 20-km radius circle is mainly phase noise left over from filtering a strong input signal. The signals from the southwest are from biological scatterers. Amount of clutter removed (difference of (a) and (b)) is shown in Figure 3 (c). As noted above, clutter removal is limited to about 50 dB due to phase noise of the transmitted signal. The clutter filter used in the adaptive setup is shown for each bin in Figure 3 (d). No filter was used in the transparent areas, 0 dB filter in the blue, 10 dB filter in the green, 30 dB filter in the yellow and 50 dB filter in the orange areas. In regions with very low reflectivity, the adaptive algorithm often varies between the unfiltered and the weakest filter choices. From a meteorological point of view this choice makes no difference because in such regions the output has little significance.
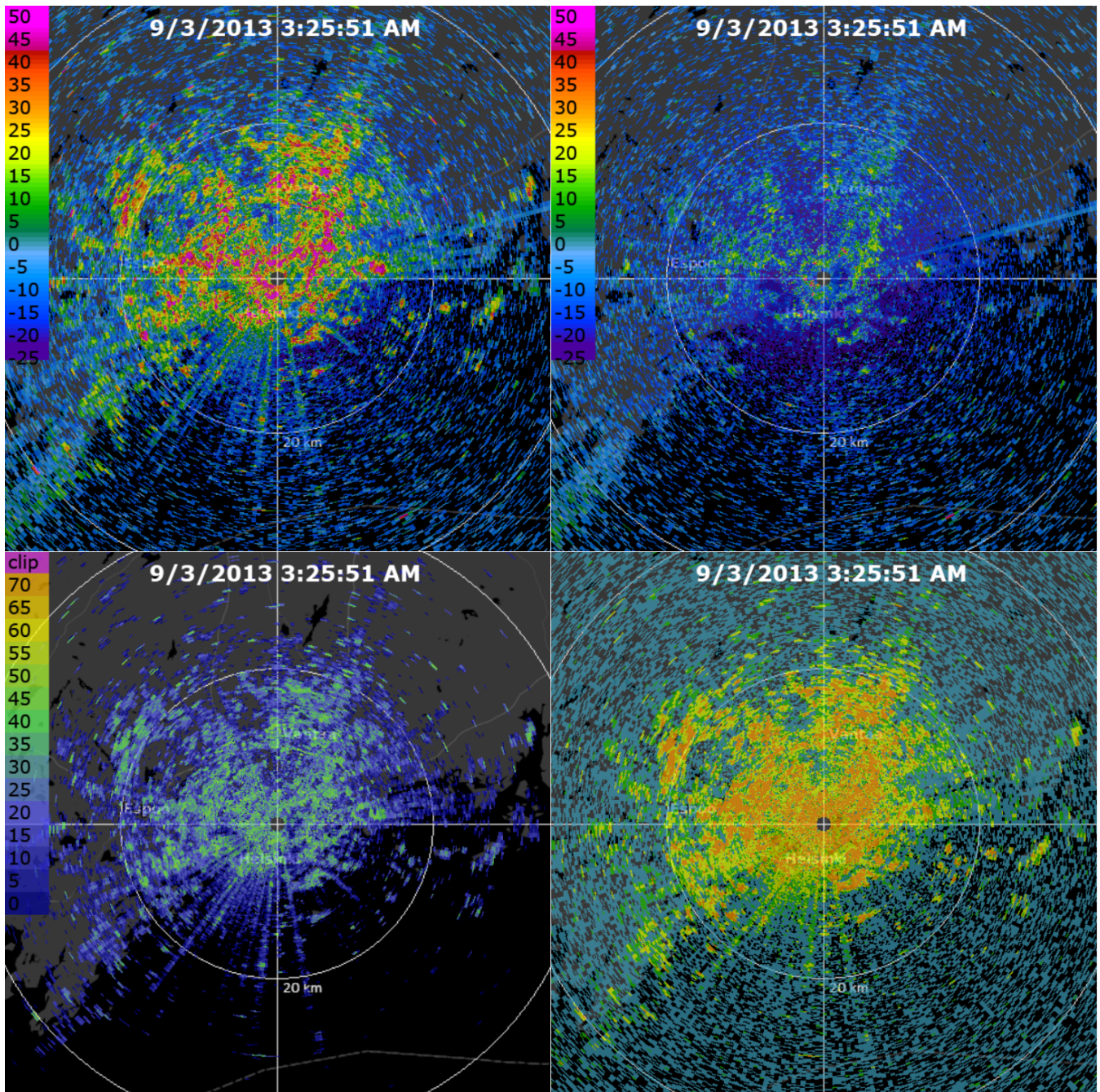
Figure 3: Clear-sky measurement: (a) received power in dBZ, (b) power after adaptive clutter filtering in dBZ, (c) amount of clutter removed in decibels, (d) clutter filter used.

In Figure 4, adaptive filtering is applied in a scan taken when heavy precipitation is passing over Helsinki region. Apart from meteorological echoes, the received power shown in Figure 4 (a) is almost the same as in the clear-sky equivalent. The difference in the low-power background in the reflectivity in Figure 4 (b) is mostly caused by insects. The suppression rate shown in Figure 4 (c) is significantly lower in regions with meteorological echoes. Also, the adaptive decision-making is usually choosing a weaker filter if meteorological reflectivity is high, as illustrated in Figure 4 (d). Note also that in regions with rain but without clutter, the adaptive decision tends to choose the unfiltered signal.
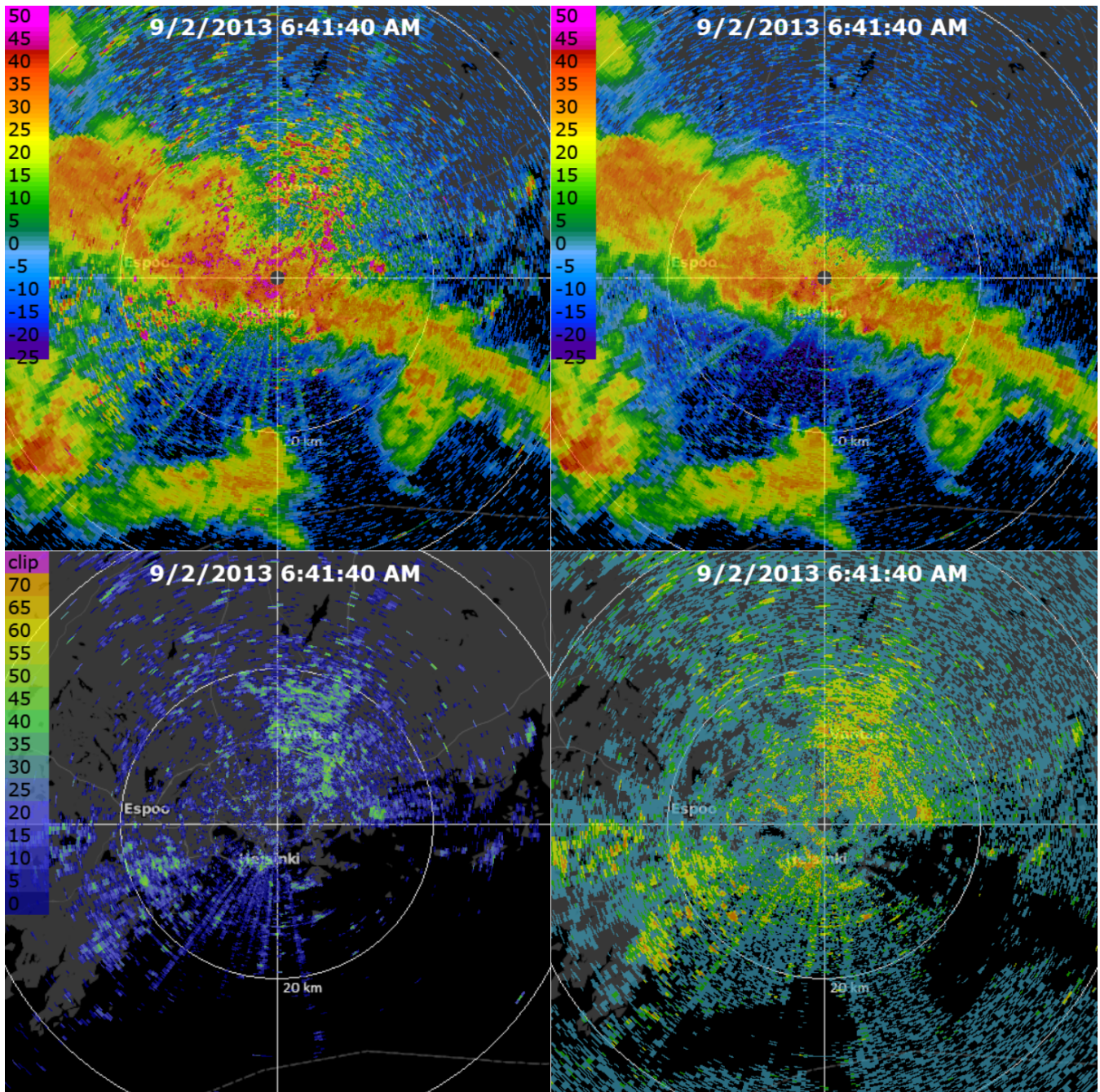
Figure 4: Measurement with heavy rain: (a) received power in dBZ, (b) power after adaptive clutter filtering in dBZ, (c) amount of clutter removed in decibels, (d) clutter filter used.

Figure 5 highlights the difference between removing clutter using a strong filter (50 dB clutter-to-signal ratio) and with the adaptive scheme. The strong filter tends to suppress meteorological echoes more than the adaptive method. Figure 5 (a) shows the difference in reflectivity obtained using adaptive and single-filter mitigation. The strong filter destroys partly the meteorological reflectivity in regions with low radial velocity, displayed in Figure 5 (b), and spectral width, displayed in Figure 5 (c). In this example the strong filter removes up to 20 decibels more than the adaptive strategy. It can be easily checked that the reflectivity difference is not due to residual clutter but suppressed precipitation by comparing the relevant polarimetric products: the copolar correlation ρ_{co} and differential phase Ψ_{dp} are essetially the same for both schemes. Too aggressive ground clutter removal often results in notable reflectivity valleys in regions around zero Doppler velocity, which are sometimes referred to as "Doppler snakes" in reflectivity. The adaptive clutter mitigation scheme avoids creating such artifacts.
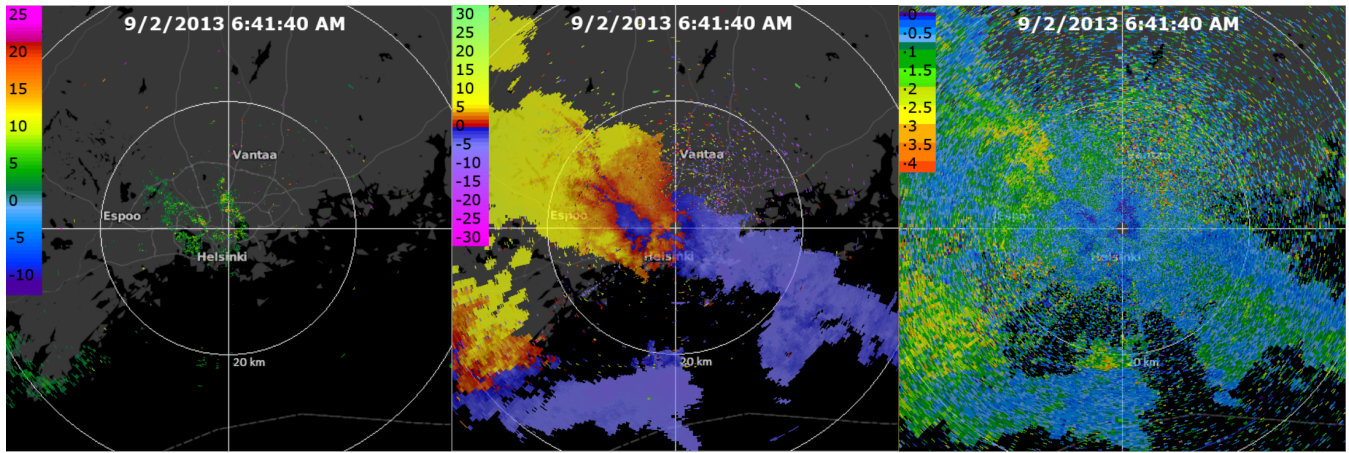
Figure 5: Adaptive and single-filter clutter removal: (a) difference in reflectivity between a 4-filter adaptive scheme and single 50 dB filter in decibels, (b) velocity in meters per second, (c) Gaussian spectral width in meters per second.

4. Conclusions

We have tested a simple adaptive clutter removal method based on an automatic polarimetric decision-making system. The algorithm is efficient enough to be applied in real time using a modern off-the-shelf PC. It is capable of removing ground clutter up to limits set by the radar, namely the phase-noise figure of the transmitted signal. Moreover, the adaptive strategy is useful in removing weak traces of ground clutter improving the quality of polarimetric products. The method is designed to avoid too aggressive filtering and related unwanted artifacts.

Acknowledgement

References

K. Friedrich, U. Germann, and P. Tabary, "Influence of ground clutter contamination on polarimetric radar parameters," 2009.

J. C. Hubbert, M. Dixon, and S. M. Ellis, "Weather radar ground clutter. part ii: Real-time identification and filtering," 2009.

C. M. Nguyen, V. Chandrasekar, and D. N. Moisseev, "Gaussian model adaptive time domain filter (gmat) for weather radars," 2008.

J. Sierwald and J. Huhtamäki, "Adaptive ground clutter removal for triple-prt setup," 2013.

——, "Triple-prt signal processing for weather radars," 2014.

A. D. Siggia and R. E. Passarelli, "Gaussian model adaptive processing (gmap) for improved ground clutter cancellation and moment calculation," 2004.

P. Tabary, F. Guibert, L. Perier, and J. Parent-du Chatelet, "An operational triple-prt doppler scheme for the french radar network," 2006.